Annals of Botany **122**: 849–860, 2018
doi: 10.1093/aob/mcy038, available online at www.academic.oup.com/aob

ANNALS OF BOTANY
Founded 1887

PART OF A SPECIAL ISSUE ON FUNCTIONAL–DEVELOPMENTAL PLANT CELL BIOLOGY

Methanol induces cytosolic calcium variations, membrane depolarization and ethylene production in arabidopsis and tobacco

Daniel Tran[1,2], Aurélien Dauphin[1,3], Patrice Meimoun[1,4], Takashi Kadono[1,5], Hieu T. H. Nguyen[6], Delphine Arbelet-Bonnin[1], Tingting Zhao[1], Rafik Errakhi[1,7], Arnaud Lehner[1,8], Tomonori Kawano[6,9,10] and François Bouteau[1,9,*]

[1]Université Paris Diderot, Sorbonne Paris Cité, Laboratoire Interdisciplinaire des Energies de Demain, Paris, France, [2]Department of Physiology & Cell Information Systems Group, McGill University, Montréal, Québec, Canada, [3]Institut Curie, CNRS UMR3215, INSERM U934, 26 rue d'Ulm, Paris 75248, France, [4]Sorbonne Université, UMR7622–IBPS, Paris, France, [5]Laboratory of Aquatic Environmental Science, Kochi University, Kochi, Japan, [6]Graduate School of Environmental Engineering, University of Kitakyushu 1-1, Hibikino, Wakamatsu-ku, Kitakyushu 808-0135, Japan, [7]Eurofins Agriscience Service, Marocco, [8]Normandie Université, UNIROUEN, Laboratoire de Glycobiologie et Matrice Extracellulaire Végétale, EA4358, SFR Normandie végétal, 76000 Rouen, France, [9]LINV Kitakyushu Research Center, Kitakyushu, Japan and [10]Université Paris Diderot, Sorbonne Paris Cité, Paris Interdisciplinary Energy Research Institute (PIERI), Paris, France
** For correspondence. E-mail francois.bouteau@univ-paris-diderot.fr*

Received: 1 December 2017 Returned for revision: 15 February 2018 Editorial decision: 23 February 2018 Accepted: 5 March 2018
Published electronically 20 March 2018

• **Background and Aims** Methanol is a volatile organic compound released from plants through the action of pectin methylesterases (PMEs), which demethylesterify cell wall pectins. Plant PMEs play a role in developmental processes but also in responses to herbivory and infection by fungal or bacterial pathogens. However, molecular mechanisms that explain how methanol could affect plant defences remain poorly understood.
• **Methods** Using cultured cells and seedlings from *Arabidopsis thaliana* and tobacco BY2 expressing the apoaequorin gene, allowing quantification of cytosolic Ca^{2+}, a reactive oxygen species (ROS) probe (CLA, *Cypridina* luciferin analogue) and electrophysiological techniques, we followed early plant cell responses to exogenously supplied methanol applied as a liquid or as volatile.
• **Key Results** Methanol induces cytosolic Ca^{2+} variations that involve Ca^{2+} influx through the plasma membrane and Ca^{2+} release from internal stores. Our data further suggest that these Ca^{2+} variations could interact with different ROS and support a signalling pathway leading to well known plant responses to pathogens such as plasma membrane depolarization through anion channel regulation and ethylene synthesis.
• **Conclusions** Methanol is not only a by-product of PME activities, and our data suggest that $[Ca^{2+}]_{cyt}$ variations could participate in signalling processes induced by methanol upstream of plant defence responses.

Key words: *Arabidopsis thaliana*, calcium, methanol, signalization, volatile

INTRODUCTION

Plant release of airborne volatile organic compounds (VOCs) in response to wounding due to pathogenic attack is well established (Engelberth *et al.*, 2004; Baldwin *et al.*, 2006; Beckers and Conrath, 2007) and plant volatile-mediated signalling is now considered for application in agriculture (Pickett and Khan, 2016). Wounding and herbivore attacks were notably shown to increase methanol emission levels, and methanol is considered as a signalling molecule within the plant and for plant–plant communication (de Gouw *et al.*, 2000; Peñuelas *et al.*, 2005; von Dahl *et al.*, 2007; Körner *et al.*, 2009; Dorokhov *et al.*, 2012). The pectin demethylation directed by pectin methylesterase (PME) is probably the main source of the methanol released in the cell wall (Nemecek-Marshall *et al.*, 1995; Fall and Benson, 1996). Cell walls are mainly composed of interacting polysaccharides, structural glycoproteins and proteoglycans, as well as proteins with multiple enzymatic activities which modify cell wall polysaccharides (Wolf and Greiner, 2012; Cosgrove, 2016). Polysaccharides are composed of three main polymers: cellulose, hemicelluloses and pectins. In the primary cell wall, cellulose is assembled into microfibrils, coated with xyloglucan interacting with other cell wall components in a complex molecular network (Carpita and Gibeaut, 1993). Thus, the plant cell wall represents a primary physical barrier against pathogens such as bacteria and fungi (Vorwerk *et al.*, 2004; Xia *et al.*, 2014). In the cell wall, the tightly packed arrangement of cellulose microfibrils makes it difficult to penetrate, leaving pectin as the prime target of pathogens (Vorwerk *et al.*, 2004). Homogalacturonan, the main pectin component, is synthesized under a highly methylesterified form which can be demethylesterified by PMEs (Wolf and Greiner, 2012). The activity of PME has a significant role in the status of pectin methylesterification, which deeply affects the pectin's properties, and could also be critical during many stages

of plant development (Wolf and Greiner, 2012; Kohli *et al.*, 2015; Li *et al.*, 2016; Huang *et al.*, 2017; Nguyen *et al.*, 2017). The pectin network is effectively disassembled at many stages during plant development, such as organ abscission and fruit ripening, and PMEs play a central role in both pectin remodelling and disassembly, and in the firming and softening of the cell wall (Duan *et al.*, 2016). Transgenic plants overexpressing a rice PME (OsPMEI28) had an increased level of cell wall-bound methylester groups and differential changes in the composition of cell wall neutral monosaccharides and lignin content leading to dwarf phenotypes (Nguyen *et al.*, 2017). However, wounding such as herbivore attack, results in drastic *de novo* PME expression, correlated to a large increase in the emission of gaseous methanol after injury (Körner *et al.*, 2009; Dorokhov *et al.*, 2012). PMEs were shown to be of critical importance for virulence, and a higher degree of cell wall methylation correlates with disease resistance in multiple plant species (Hasunuma *et al.*, 2003; Lionetti *et al.*, 2007, 2017; Reignault *et al.*, 2008; Raiola *et al.*, 2011; Volpi *et al.*, 2011). Pathogens could also regulate the expression of certain plant PMEs that results in increasing both susceptibility to the pathogen and methanol release (Peñuelas *et al.*, 2005; von Dahl *et al.*, 2006; Körner *et al.*, 2009; Raiola *et al.*, 2011; Lionetti *et al.*, 2012). This is consistent with the increased resistance against herbivores of transgenic tobacco plants overexpressing PMEs and overproducing methanol (Dixit *et al.*, 2013). PME-generated methanol release from wounded plants was shown to upregulate defence genes and active defensive reactions of neighbouring plants, allowing resistance to the bacterial pathogen (Dorokhov *et al.*, 2012; Komarova *et al.*, 2014).

Direct spraying of methanol onto leaves of *Arabidopsis thaliana* seedlings was shown to regulate the expression of 484 genes involved in signalling, defence, metabolism (especially flavonoid metabolism) and detoxification (Downie *et al.*, 2004). Taken together, these data effectively indicate that methanol is not only a by-product of PME activity, but could also act as an interplant alarm signal. However, the mechanism by which methanol activates signalling pathways that translate the methanol signal into an output defence response has yet to be determined. The cytosolic free Ca^{2+} concentration ($[Ca^{2+}]_{cyt}$) in plant cells frequently changes rapidly and dynamically in response to pathogen attacks (Lecourieux *et al.*, 2006; Ma *et al.*, 2011; Zhang *et al.*, 2014). Such $[Ca^{2+}]_{cyt}$ variations could be promoted by various volatiles with different kinetic patterns and intensities, depending on the nature of the volatile (Asai *et al.*, 2009; Zebelo *et al.*, 2012). Elevations in $[Ca^{2+}]_{cyt}$ are sensed by Ca^{2+}-binding proteins (calmodulin, calcium-dependent protein kinases or calcineurin B-like proteins) which relay or decode the encoded Ca^{2+} signals into specific cellular and physiological responses in order to survive pathogen attacks (Zhang *et al.*, 2014). We thus tested whether methanol could induce $[Ca^{2+}]_{cyt}$ variations in cultured cells and seedlings and then looked to see whether these variations could be related to some classical plant defence responses, namely reacive oxygen species (ROS) generation, ion flux regulation and ethylene synthesis (Wu *et al.*, 2014).

MATERIALS AND METHODS

Suspension cell cultures

Arabidopsis thaliana L. (Col-0) suspension cells and *Nicotiana tabacum* (BY-2) cell suspensions containing recombinant apoaequorin targeted to the cytosol were grown at pH 5.8 in Gamborg medium and Murashige and Skoog (MS) medium, respectively. They were maintained at 24 ± 2 °C, under continuous darkness and continuous shaking (on a gyratory shaker) at 120 rpm. Suspension cells were sub-cultured weekly using 1:10 and 1:40 dilutions for *A. thaliana* and tobacco, respectively. All experiments were performed at 22 ± 2 °C using log-phase cells (4 and 6–7 d after sub-culture for *A. thaliana* cells and tobacco cells, respectively).

Seedling culture

Arabidopsis thaliana L. ecotype Wassilewskija (Ws) seeds containing recombinant cytosolic apoaequorin were sterilized in 1 % (w/v) sodium hypochlorite, and allowed to germinate on sterilized MS agar plates containing vitamin B5 but lacking 2,4-dichlorophenoxy acetic acid (2,4-D). The seedlings were grown on the agar plates under a 12/12 h under dark/light regime (45 µmol m^{-2} s^{-1}) for 20 d at 22 ± 2 °C.

Cytosolic calcium measurements

Cell suspensions of *A. thaliana* and tobacco, or *A. thaliana* seedlings expressing apoaequorin in the cytosol were used to record cytoplasmic Ca^{2+} variations (Knight *et al.*, 1991). Aequorin was reconstituted by overnight incubation of the cell suspensions or seedlings in Gamborg or MS medium containing 12.5 µM native coelenterazine. For cell suspensions, 500 µL aliquots of cell suspension were directly transferred carefully to a luminometer glass tube. Treatments with non-lethal amounts of methanol (Supplementary Data Fig. S1) were performed by gentle pipette injection in the luminometer tubes. To record the effect of volatile methanol on seedlings, after aequorin was reconstituted, one seedling was carefully transferred on the upper part of a luminometer glass tube (their wet status allowing the seedling to adhere to the tube wall). Then various amounts of methanol were able to become volatile when added with the pipette on a small cotton puff placed in the bottom of the luminometer tube, which was then tightly sealed with parafilm. The luminescence counts were recorded continuously at 0.2 s intervals with a FB12-Berthold luminometer. At the end of each experiment, the residual aequorin was discharged by addition of 1 mL of a 1 M $CaCl_2$ solution dissolved in 100 % methanol. The resulting luminescence was used to estimate the total amount of aequorin for each condition. Calibration of calcium levels was performed using the equation: $pCa = 0.332588(-\log k) + 5.5593$, where k is a rate constant equal to luminescence counts per second divided by total remaining counts (Knight *et al.*, 1996). Data are expressed as micromolar and are means ± s.e.

Electrophysiology

Individual *A. thaliana* cultured cells were impaled in the culture medium with borosilicate capillary glass (Clark GC 150F) micropipettes (resistance: 50 MΩ when filled with 600 mM KCl). The main ion concentrations in the Gamborg medium after 4 d were 9 mM K^+ and 11 mM NO_3^- (Reboutier *et al.*, 2002). Individual cells were voltage-clamped using an Axoclamp 2B amplifier (Axon Instruments, Foster City, CA, USA) for discontinuous single electrode voltage clamp

(dSEVC) experiments as previously described (Reboutier *et al.*, 2002; Errakhi *et al.*, 2008*a*, *b*; Tran *et al.*, 2013). Voltage and current were digitized using a computer fitted with a Digidata 1320A acquisition board (Axon Instruments). The electrometer was driven by pClamp software (pCLAMP8, Axon Instruments). Data are expressed as milliVolts or percentages, and are means ± s.e.

Monitoring of ROS production

The production of ROS was monitored by the chemiluminescence of the *Cypridina* luciferin analogue (CLA) as previously described (Kadono *et al.*, 2010; Tran *et al.*, 2013). CLA is known to react mainly with $O_2^{\cdot -}$ and $^1O_2$ with light emission (Nakano *et al.*, 1986). Chemiluminescence from CLA was monitored using a FB12-Berthold luminometer with a signal integrating time of 0.2 s. The ROS scavengers 1,2-dihydroxybenzene-3,5-disulphonic acid disodium salt (Tiron) and 1,4-diazabicyclo[2.2.2]octane (DABCO) were added 20 min prior to methanol treatment.

Ethylene measurement

A 2.5 mL aliquot of tobacco cell suspension was sub-cultured in 5 mL flasks tightly closed with serum caps, maintained at 22 °C under constant shaking. After 2 h, a 2 mL gas sample was taken from each flask and injected into a gas chromatograph (GC) (Hewlet Packard 5890 series II) equipped with a flame ionization detector (FID) and an activated alumina column (6 mm in internal diameter, 50 cm long, 50–80 mesh) for ethylene determination (Errakhi *et al.*, 2008*a*). Results are presented as the means of 3–6 measurements ± s.e. and are expressed as picomoles of ethylene produced per 1 g of fresh matter.

Determination of vaporized methanol

Vaporized methanol samples were analysed using a GC (Shimadzu GC-2014, Tokyo, Japan) with FIDs, fitted with a packed column (Porapak-Q 50/80), equipped with a C-R8A Chromatopac Data Processor (Shimadzu, Tokyo, Japan). Temperatures at the injection ports, column and detectors were maintained at 150, 80 and 200 °C, respectively. The flow rate of carrier gas (N_2) was 50 mL min^{-1}. The retention time for the methanol peak was 5.75 min. For calibration, standard methanol vapour (22.4 %, v/v) was prepared by evaporating the drops (32 µL) of liquid methanol under vacuum at 100°C in the 100 mL gas-sampling bottle. Vaporized methanol samples were mixed with fresh air and injected to a GC. In order to estimate the methanol vapour concentration derived from liquid methanol in the sealed 3.5 mL glass tubes (with plant seedlings hanging on the inner wall), a specific model container allowing both passive evaporation of methanol from the liquid methanol droplet applied onto the cotton puff, and collection of an air sample without altering the inner pressure was designed. Sampled air was used for methanol determination with GC. Evaporation of methanol (10 µL, liquid) was allowed for 0.25, 0.5, 1, 2, 5, 10, 15, 30 and 60 min, and the temporal profile of methanol evaporation was monitored.

Statistics

Significant differences between treatments were determined by the Mann–Whitney test, and *P*-values <0.05 were considered significant.

RESULTS

Methanol induced a biphasic variation of cytosolic Ca^{2+} *in cultured cells*

Addition of methanol induced a rapid biphasic variation of $[Ca^{2+}]_{cyt}$ composed of an early peak followed by a second slower transient increase in *A. thaliana* cells (Fig. 1A) and tobacco cells (Supplementary Data Fig. S3A). The first and the second peaks of $[Ca^{2+}]_{cyt}$ appeared to be dose dependent, both increasing after addition of 0.1–5 % methanol in *A. thaliana* cells (Fig. 1B). The methanol-induced first short-lived increase in $[Ca^{2+}]_{cyt}$ could be reduced upon a 20 min pre-treatment with a plasma membrane (PM) Ca^{2+} channel blocker, lanthanum (500 µM $LaCl_3$) (Fig. 1C, D; Supplementary Data Fig. S2C, D) or a Ca^{2+} chelator 1,2-bis(*o*-aminophenoxy)ethane-*N*,*N*,*N*,*N*-tetraacetic acid (1 mM BAPTA) (Fig.1C, D). The second peak of $[Ca^{2+}]_{cyt}$ was even more reduced, by about 80 %, after such pre-treatments (Fig. 1C, D; Supplementary Data Fig. S3B). In order to assess the possible involvement of Ca^{2+} intracellular stores in the methanol-induced variations in $[Ca^{2+}]_{cyt}$, cells were incubated with dantrolene and 8-bromo-cADP-ribose (8-Br-cADPr), ryanodine receptor (RyR) agonists, or caffeine, that allows depletion of the intracellular Ca^{2+} store, 20 min prior to methanol treatment. The level of the second methanol-induced increase in $[Ca^{2+}]_{cyt}$ was inhibited by >70 % with caffeine, dantrolene and 8-Br-cADPr, whereas the first rapid variation was only slightly reduced (Fig. 1C, D). These data indicated that methanol could induce a complex calcium signalling pathway, involving different source of Ca^{2+} in plant cells.

Ca^{2+} *influx is an upstream event of methanol-induced depolarization of plant cells*

Variations of cell polarization and anion currents are some of the earliest signalling events detectable upon plant–pathogen interactions (Errakhi *et al.*, 2008*a*; Wu *et al.*, 2014) or volatile application (Zebelo *et al.*, 2012). Thus, methanol's effects were further tested on cell polarization and anion currents using dSEVC on *A. thaliana* cultured cells. As reported by previous dSEVC studies (Errakhi *et al.*, 2008*a*; Kadono *et al.*, 2010; Tran *et al.*, 2013), in control conditions, cultured cells display whole-cell currents being mainly carried by anion currents, which are the main hallmarks of slow anion channels (Reboutier *et al.*, 2002) and were sensitive to unrelated anion channel inhibitors (Reboutier *et al.*, 2002, 2005; Kadono *et al.*, 2010). This explains the value of the resting membrane potential (V_m) of –40 ± 5 mV (n = 25) as previously reported (Reboutier *et al.*, 2002; Haapalainen *et al.*, 2012; Tran *et al.*, 2013). However, in these conditions, addition of methanol induced a depolarization of the cell PM, reaching its maximal amplitude within about 1 min, followed by a repolarization to the control level (Fig. 2A). These transient variations of membrane potential (V_m) were dose dependent, being significant from 1 % methanol (Fig. 2A, B). Methanol also induced a transient increase in anion current of –1.22 ± 0.55 nA (n = 5) for 5

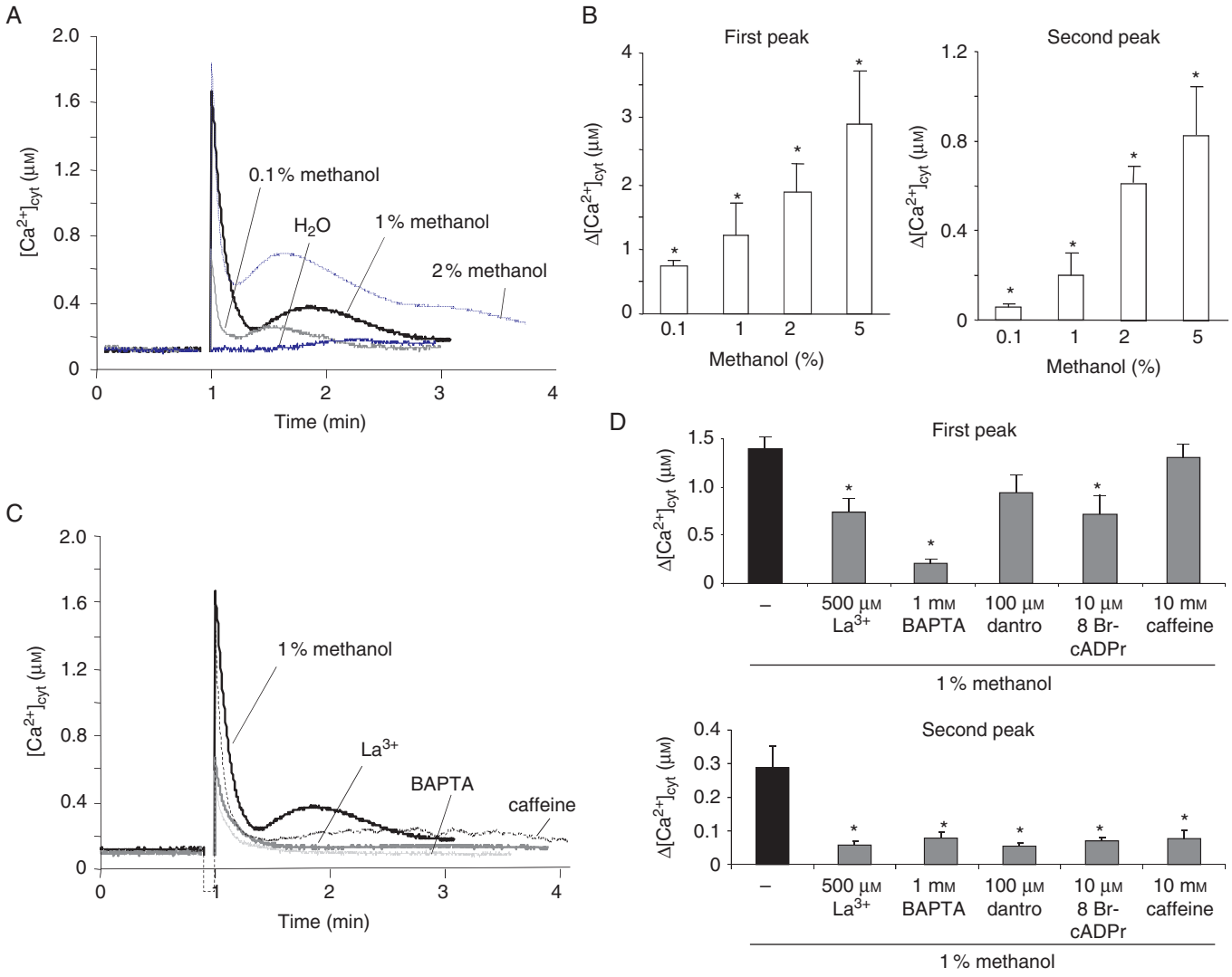

FIG. 1. Effect of methanol on the cytosolic Ca^{2+} concentration in cultured cells. (A) Typical changes in $[Ca^{2+}]_{cyt}$ measured by using cell suspensions derived from *A. thaliana* transformed by the apoaequorin gene upon addition of various concentrations of methanol ranging from 0.1 to 2 % (0.5–10 µL in 500 µL of Gamborg medium). (B) Mean values of $\Delta[Ca^{2+}]_{cyt}$ for the first and the second peak depending on the volume of methanol added. *Significantly different from the control level (addition of 25 µL of H_2O). (C) Changes in $[Ca^{2+}]_{cyt}$ induced by 5 % (v/v) methanol after pre-treatment with the Ca^{2+} channel inhibitor (500 µM La^{3+}), the calcium chelator (1 mM BAPTA) or caffeine (10 mM) allowing depletion of the Ca^{2+} internal stores. (D) Mean values of methanol-induced $\Delta[Ca^{2+}]_{cyt}$ on the first and second peak after pre-treatment with 500 µM La^{3+}, 1 mM BAPTA, 10 mM caffeine or inhibitors of endomembrane Ca^{2+}-permeable channels (100 µM dantrolene and 10 µM 8 bromo-cADPr). Data correspond to the means of at least five independent experiments ± s.d. *Significantly different from the $[Ca^{2+}]_{cyt}$ variation induced by 1 % methanol. (A) and (C) are presented with an extended scale in Supplementary Data Fig. S2 for a better resolution of the firts peaks.

% methanol (Fig. 2C, D) from a control value of –0.95 ± 0.15 nA (n = 15). Upon repolarization of the cells, the anion current level decreased to the control level recorded before methanol addition (Fig. 2C). The transient regulation of these currents certainly explains the observed transient depolarization. Pre-treatment of the cells with La^{3+} or BAPTA abolished the methanol-induced increase in anion currents and depolarization (Fig. 2B, D). This indicates that the cytosolic increase in Ca^{2+} is an upstream event, when compared with methanol-induced anion current regulation and PM depolarization.

Interaction between methanol-induced ROS generation and Ca^{2+} variations in cultured cells

The ROS generation induced by methanol was characterized using tobacco cells. Addition of methanol (1–5 %) induced a dose-dependent short-lived increase in ROS (Fig. 3A) that could be abolished upon a pre-treatment with DABCO, a scavenger of singlet oxygen ($^1O_2$) (Fig. 3B). This first peak could be followed by a second slower transient increase (Fig. 3B). Tiron, a scavenger of superoxide anion ($O_2^{\cdot -}$), failed to decrease the early short-lived increase in ROS (Fig. 3B). In the set of experiments in which a second increase in ROS was recorded, this increase was reduced by DABCO but also by Tiron. The first early peak of ROS could not be reduced by La^{3+} or BAPTA, but these inhibitors decreased the second increase in ROS (Fig. 3B). These data suggest that methanol could induce a rapid increase in $^1O_2$ and a slightly delayed increase in $O_2^{\cdot -}$, the latter possibly being dependent on the early induced $^1O_2$ generation and Ca^{2+} influx.

Therefore, we tested the impact of this ROS pharmacology on the methanol-induced $[Ca^{2+}]_{cyt}$ variations. DABCO, the scavenger of $^1O_2$, almost eliminated the first and second peak of

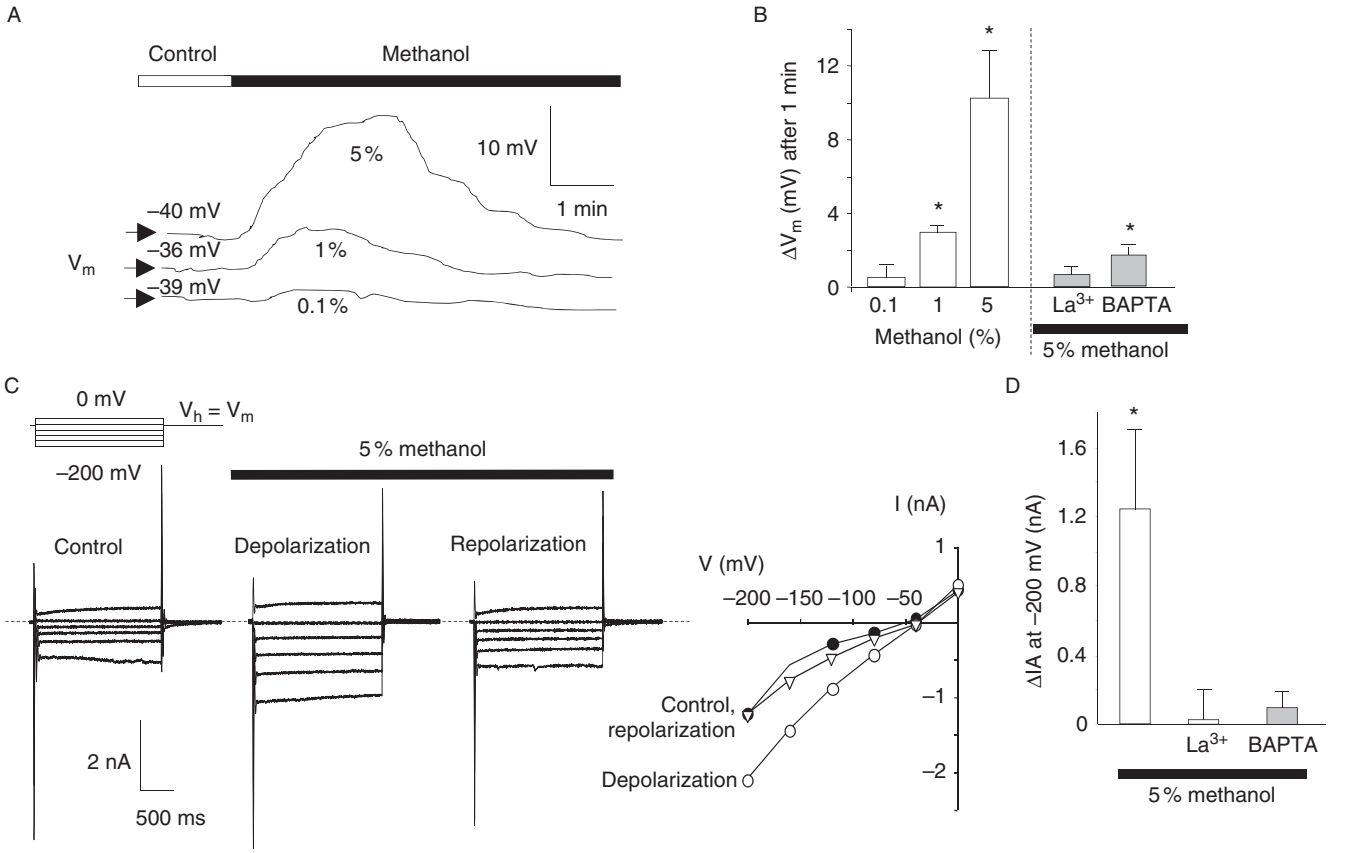

FIG. 2. Methanol-induced transient changes in membrane potential and anion current of cultured cells. (A) Typical recording of the membrane potential (V_m) of an *A. thaliana* cultured cell after addition of methanol. The bar illustrates the time when methanol was added to the 500 µL of Gamborg medium. (B) Mean values of the maximal depolarization upon addition of various doses of methanol or after pre-treatment with the Ca^{2+} channel inhibitor (500 µM La^{3+}) or the calcium chelator (1 mM BAPTA). (C) Typical methanol-induced changes in anion currents (recorded using dSEVC) during depolarization and repolarization, and corresponding current–voltage curves (V_h = holding potential, V_m = membrane potential). (D) Mean values of anion current increases (recorded 1.9 s after the imposition of a –200 mV pulse) at the maximal depolarization induced by 5 % methanol alone or after pre-treatment with 500 µM La^{3+} or 1 mM BAPTA. Results are presented as means of at least five measurements ± s.d. *Significantly different from the control level recorded before methanol addition.

Ca^{2+} (Fig. 3C), suggesting that the rapid $^1O_2$ generation could be an upstream event even when compared with the methanol-induced Ca^{2+} variations. On the other hand, Tiron, the scavenger of $O_2\cdot^-$, decreased the methanol-induced increases in $[Ca^{2+}]_{cyt}$ (Fig. 3C), indicating that $O_2\cdot^-$ generation could also participate in the methanol-induced $[Ca^{2+}]_{cyt}$ variations, implying complex interactions between ROS generation and $[Ca^{2+}]_{cyt}$ variations.

Methanol induced a calcium-dependent ethylene production in cultured cells

Methanol was notably shown to induce an increase in gene expression of the ethylene biosynthetic enzyme 1-aminocyclopropane-1-carboxylate (ACC) oxidase (Downie *et al.*, 2004). We thus investigated eventual methanol-induced ethylene synthesis and its dependence on Ca^{2+} influx in cultured cells. Accumulation of ET was observed in the cell culture flask, reaching 60 % with 1 % methanol after 4 h (Fig. 4) and 300 % with 5 % methanol (not shown). Pre-treatment of suspension cells by α-aminoisobutyric acid (AIB), an inhibitor of ACC oxidase, or by aminooxyacetic acid (AOA), an inhibitor of ACC synthase, at 200 µM each, for 4 h inhibited the ethylene synthesis induced by methanol (Fig. 4). The addition of BAPTA or La^{3+} reduced the methanol-induced ethylene synthesis, indicating that the cytosolic Ca^{2+} increase is an upstream event in the pathway leading to ethylene synthesis (Fig. 4).

Volatile methanol induced [Ca²⁺]cyt variations in A. thaliana *seedlings*

To assess further the impact of methanol on Ca^{2+} signalling in plants, we examined the time-course of the volatile methanol-induced increase in $[Ca^{2+}]_{cyt}$ in *A. thaliana* seedlings. Different amounts of liquid methanol were dropped on a cotton puff in the bottom of the luminometer tubes, allowing the release of gaseous methanol to seedlings placed on the upper part of the tubes. Volatile methanol promoted increases in $[Ca^{2+}]_{cyt}$ with different kinetic patterns and intensities for methanol volumes >1 µL (Fig. 5A). However, the maximal increases in $[Ca^{2+}]_{cyt}$ seemed to be dose dependent, along with the increased concentration of vaporized methanol determined at the 15 min time point [and not dependent on the added methanol volumes (Fig. 5B)]. Note that we have preliminarily examined the temporal profile of passive methanol vaporization from liquid methanol (10 µL) dropped onto a cotton puff placed on the bottom of a sealed tube (3.5 mL),

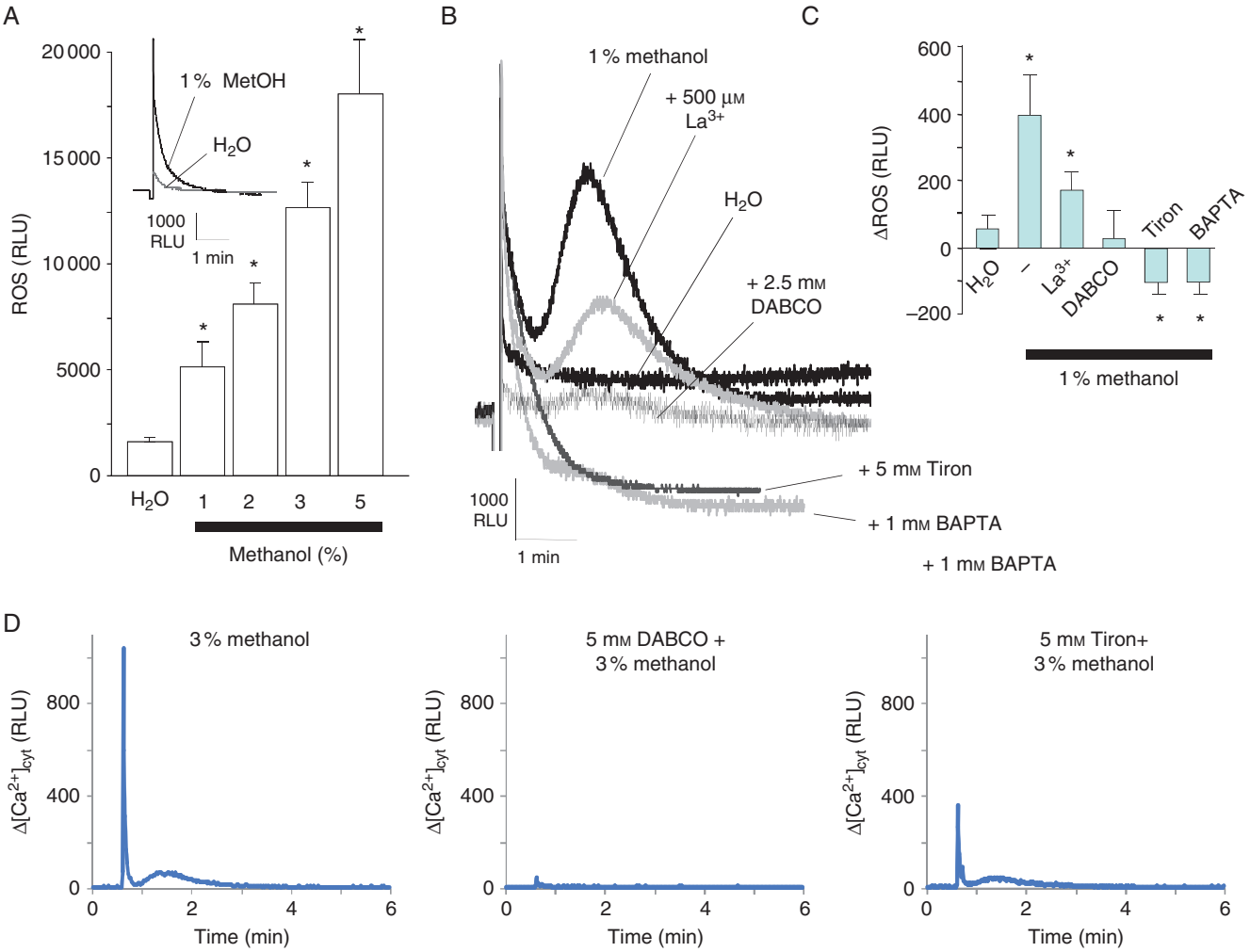

FIG. 3. Methanol-induced reactive oxygen species (ROS) generation in BY2 cultured cells. (A) Mean values of fast ROS generation in tobacco cells upon addition of methanol ranging from 0.1 to 5 % (v/v). Typical kinetics of the fast ROS generation are presented in the inset. (B) Mean biphasic ROS generation induced by methanol (1 %) and effects of pre-treatments with a Ca^{2+} channel inhibitor (500 µM La^{3+}), a calcium chelator (1 mM BAPTA), a scavenger of $^1O_2$ (2.5 mM DABCO) or a scavenger of $O_2^{\cdot-}$ (Tiron 5 mM). (C) Quantification of the second ROS peak. (D) Effect of DABCO and Tiron on the changes in $[Ca^{2+}]_{cyt}$ induced by 3 % methanol. Results are presented as means of at least five measurements ± s.d. *Significantly different from the control level (addition of 25 µL of H_2O). (B) is presented with an extended scale in Supplementary Data Fig.S6 for a better resolution of the first peaks.

attaining a saturated level (approx. 14 %, v/v) within an initial 1–2 min (data not shown).

In order to discriminate between the impact of volatile methanol on aerial parts and on roots, seedlings were incised and incubated overnight with coelenterazine to adapt the root and leaf parts after mechanical damage due to incision. Although shorter, the luminescence recorded for the aerial parts appeared more important than that observed from roots (Fig. 6), suggesting that the volatile methanol-induced increase in $[Ca^{2+}]_{cyt}$ in seedlings was mainly due to the leaves.

DISCUSSION

It is well established that Ca^{2+} is a ubiquitous secondary messenger for cellular signalling in various stresses comprising plant immune responses (Lecourieux *et al.*, 2006; Ma *et al.*, 2011; Seybold *et al.*, 2014). Cytosolic Ca^{2+} variations were also reported in volatile-sensing mechanisms (Walter *et al.*, 2007; Chen *et al.*, 2008; Asai *et al.*, 2009; Zebelo *et al.*, 2012; Zhang *et al.*, 2015), but to our knowledge nothing was reported on methanol, although it was shown to upregulate defence genes and active defensive reactions (Dorokhov *et al.*, 2012; Komarova *et al.*, 2014). In this study, we showed that exogenous methanol could induce $[Ca^{2+}]_{cyt}$ increases in plant cells when applied in the liquid phase or as a volatile. The methanol released in the demethylation of pectin splits into the gas and liquid phases according to Henry's Law, methanol emissions in leaf reflecting a dynamic balance between rates of production, phase partitioning, stomatal conductance and transpiration (Harley *et al.*, 2002). The biphasic kinetics of the $[Ca^{2+}]_{cyt}$ increases recorded when methanol was applied in the liquid phase for the suspension cells (Fig. 1A; Supplementary Data Fig. S3A) or seedlings (Supplementary Data Fig. S4A) were more reproducible when compared with volatile methanol applications which displayed more chaotic kinetics (Fig. 5). Root cells seemed less sensitive than leaf cells (Fig. 6), perhaps due to the lack of an effective pathway for processing methanol in roots (Ramirez *et al.*, 2006).

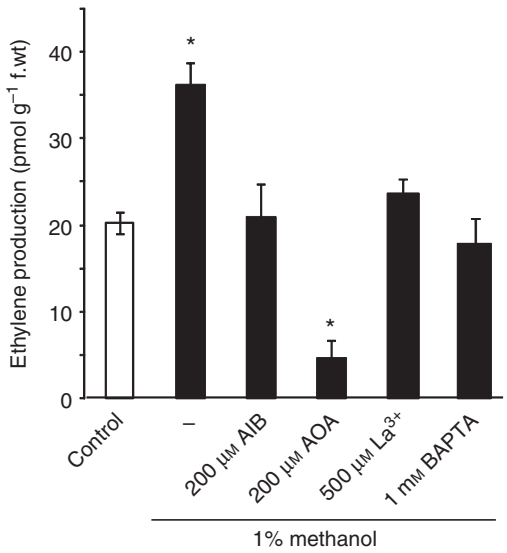

FIG. 4. Methanol-induced ethylene synthesis in cultured cells. Methanol-induced synthesis of ethylene in tobacco cells after a 4 h treatment and its inhibition by pre-treatment with 200 µM α-aminoisobutyric acid (AIB), an inhibitor of ACC oxidase, or 200 µM aminooxyacetic acid (AOA), an inhibitor of ACC synthase. Pre-treatment with a Ca^{2+} channel inhibitor (500 µM La^{3+}) or a calcium chelator (1 mM BAPTA) also reduced the methanol-induced ethylene production after 4 h. Data are expressed as picomoles of ethylene produced per gram of fresh weight, and are representative of at least four independent experiments, and error bars correspond to the standard errors. *Significantly different from the control level (addition of 5 µL H_2O).

However, these $[Ca^{2+}]_{cyt}$ increases could be minimized upon pre-treatment with the PM Ca^{2+} inhibitor La^{3+} when methanol was added in the liquid phase for suspensions cells and seedlings (Figs 1C, D and 3D; Supplementary Data Fig. S3) or as a volatile (Supplementary Data Fig. S5), indicating a rapid influx of Ca^{2+} through PM Ca^{2+} channels upon methanol challenge. The first and second peak delayed Ca^{2+} increases observed upon addition of liquid methanol could also be reduced by the Ca^{2+} chelator BAPTA, reinforcing the apoplast as a source of Ca^{2+} in this process. It is noteworthy that Ca^{2+} was shown to be mobilized from an apoplastic source to contribute to the increase in $[Ca^{2+}]_{cyt}$ level during PME activity (Wu and Jinn, 2010). Thus activation of PME upon pathogen attacks that leads to methanol production (de Gouw *et al.*, 2000; Peñuelas *et al.*, 2005; von Dahl *et al.*, 2007; Körner *et al.*, 2009; Dorokhov *et al.*, 2012) and remobilization of apoplastic Ca^{2+} could lead to $[Ca^{2+}]_{cyt}$ increases. However, the $[Ca^{2+}]_{cyt}$ increases induced by methanol (mainly the second) were also reduced by dantrolene and 8 bromo-cADPr, inhibitors of endomembrane Ca^{2+}-permeable channels (RyR-like channels) and by caffeine allowing depletion of the Ca^{2+} internal stores, suggesting that methanol also promotes Ca^{2+} release from intracellular stores. The inhibition of both fast and delayed Ca^{2+} increases by La^{3+} and BAPTA and the inhibition of the delayed Ca^{2+} increase by an inhibitor of internal Ca^{2+} store release suggests a possible Ca^{2+}-induced Ca^{2+} release involving PM Ca^{2+} channels that induced a Ca^{2+} release from internal stores (Bewell *et al.*, 1999), as already reported in response to various stimuli in plants (Meimoun *et al.*, 2009*a*; Liu *et al.*, 2012). It is further noteworthy that $[Ca^{2+}]_{cyt}$ increases were higher in *A. thaliana* cultured cells than in BY2 tobacco cells, suggesting a stronger sensitivity of *A. thaliana* cells to methanol, as already reported with thaxtomin A, a toxin inducing Ca^{2+} influx (Meimoun *et al.* 2009*b*).

Generation of ROS is postulated to be an integral part of the defence responses of the plant (Lehmann *et al.*, 2015; Camejo *et al.*, 2016) that frequently interacts with Ca^{2+} signalling (Kadono *et al.*, 2010; Frederickson Matika and Loake, 2014). In response to methanol, we could effectively record a very fast dose-dependent $^1O_2$ generation in suspension cells (Fig. 3) and seedlings (Supplementary Data Fig. S6). The inhibition of this fast $^1O_2$ production allowed elimination of all the $[Ca^{2+}]_{cyt}$ variations, this $^1O_2$ production thus appearing as the earliest methanol-induced response we could record. As expected from an $^1O_2$-dependent $[Ca^{2+}]_{cyt}$ elevation, BAPTA and La^{3+} were inefficient in reducing the $^1O_2$ production which is an upstream event. Such fast $^1O_2$ production responsible for activation of Ca^{2+} influx through PM channels was already reported in response to salt stress in various plant cells (Monetti *et al.*, 2014; Ben Hamed *et al.*, 2016). The origin of this fast $^1O_2$ production remains unclear, and we cannot even exclude the production of $O_2^{\cdot -}$ in this fast ROS generation, since Tiron, a scavenger of $O_2^{\cdot -}$, could also reduce the fast $[Ca^{2+}]_{cyt}$ variations, although less efficiently. NADPH-oxidases such as AtRbohD and AtRbohB (for respiratory burst oxidase homologue), known to participate in plant–pathogen interactions (Pogány *et al.*, 2009; Nagano *et al.*, 2016), are not the source of this fast early ROS generation since it was still recorded in response to methanol in *A. thaliana* RBOH mutants *AtrbohD and AtrbohB*, and the double mutant *AtrbohB-D* (Supplementary Data Fig. S7A). The mechanism at the origin of this early ROS generation is still to be determined. Several cell wall-located enzymes such as polyamine oxidases (Pottosin and Shabala, 2014) or peroxidases (Kimura and Kawano, 2015) that could be responsible for extracellular $^1O_2$ generation (Kawano *et al.*, 1998; Kanofsky, 2000; Guo *et al.*, 2009) are known to be responsible for cell wall ROS production susceptible to control of Ca^{2+} transport across the PM.

However, inhibiting this fast ROS generation also allowed inhibition of the delayed $O_2^{\cdot -}$ generation, as it could be observed with BAPTA and La^{3+}. These data suggest that the delayed $O_2^{\cdot -}$ generation was dependent on the $[Ca^{2+}]_{cyt}$ variations, highlighting a complex interplay between generation of different ROS and $[Ca^{2+}]_{cyt}$ variations (Fig. 7). These data are reminiscent of what was observed upon salicylic acid treatment (Kimura and Kawano, 2015) for which apoplastic peroxidases are likely to be involved in the earlier phase of oxidative burst, and NADPH oxidases are likely to be involved in the late phase of the oxidative burst, the key signalling event connecting the two phases of oxidative burst being calcium channel activation. Although methanol alone was not shown to be active on ROS generation in tomato, only allowing the increase and prolongation of the flg22-induced oxidative burst (Hann *et al.*, 2014), our data reinforced the hypothesis of a role for methanol in inducing a signalling pathway. Effectively, ROS generations (in addition to $[Ca^{2+}]_{cyt}$ variations) belong to early events responsible for most of the ensuing cascades of chemical and molecular reactions leading to plant defence response (Maffei *et al.*, 2007). We cannot exclude that methanol-induced ROS generation may locally modify the cell wall plasticity. It has been shown that ROS, particularly hydroxyl radicals, may modify the cell wall plasticity (Fry *et al.*, 2001; Schopfer, 2001; Tenhaken, 2015). It

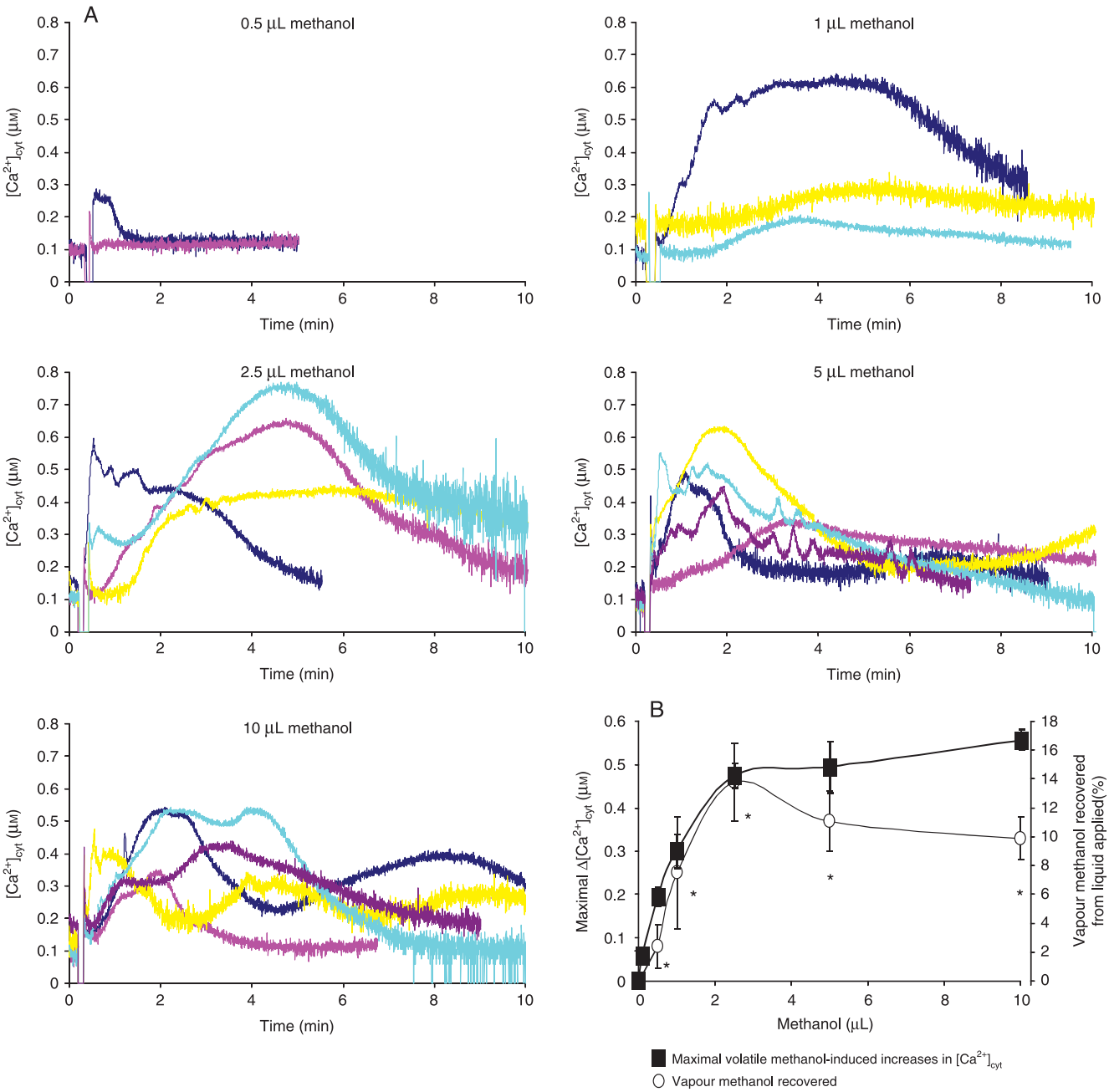

FIG. 5. Effect of volatile methanol on cytosolic Ca^{2+} concentrations of seedlings. (A) Changes in $[Ca^{2+}]_{cyt}$ were measured by using seedlings from *A. thaliana* transformed by the apoaequorin gene. Different amounts of liquid methanol (0.5–10 µL) were dropped on a cotton puff in the bottom of the luminometer tubes, allowing the release of gaseous methanol to seedlings. (B) Maximal volatile methanol-induced increases in $[Ca^{2+}]_{cyt}$ and vapour methanol recovered reported as a function of applied liquid methanol. Data correspond to the means of at least three independent experiments ± s.d. *Significantly different from the control level before methanol addition.

is also known that demethylesterified homogalacturonan can form ionic bonds between the negatively charged carboxyl groups of several homogalacturonan chains and Ca^{2+} ions, forming a pectate gel that may provide sufficient stiffness to delay the progression of the pathogen.

We also observed that methanol could regulate anion currents through the PM, another rapid signalling event frequently detected upon plant–pathogen interactions (Errakhi *et al.*, 2008*a*, *b*; Wu *et al.*, 2014). Methanol could effectively induce a transient cell depolarization due to the activation of anion channels. These responses were blocked by La^{3+} and BAPTA, highlighting their dependence on $[Ca^{2+}]_{cyt}$ variations, as already reported in response to thaxtomin and ozone (Errakhi *et al.*, 2008*b*; Kadono *et al.*, 2010). Partly recovered rapid depolarizations have already been recorded in tomato upon challenge with leaf-emitted volatiles (Zebelo *et al.*, 2012), but their role in VOC-induced signalling was not shown. Here we showed that the methanol-induced regulation of anion channels could participate in the pathway leading to ethylene production since it was reduced by glibenclamide and 9AC, two structurally

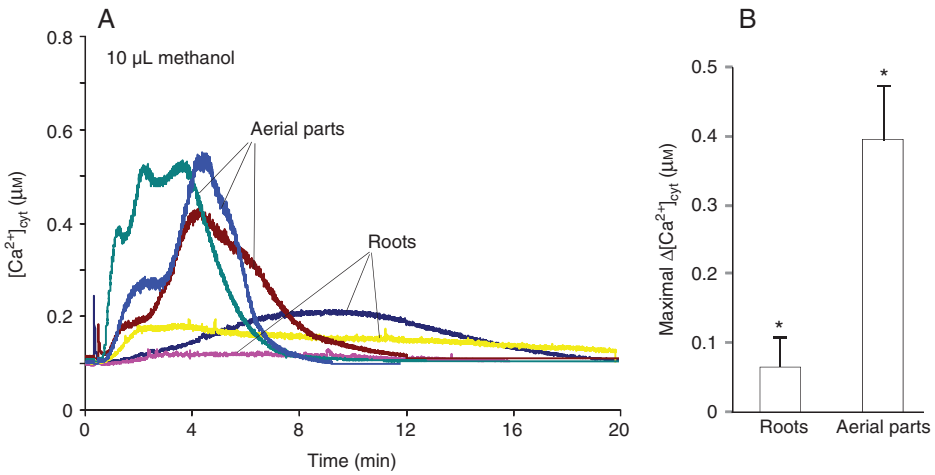

FIG. 6. Effect of volatile methanol on cytosolic Ca^{2+} concentrations in roots and aerial parts of seedlings. (A) Changes in $[Ca^{2+}]_{cyt}$ were measured by using only roots or aerial parts of excised seedlings from *A. thaliana* transformed by the apoaequorin gene. A 10 µL aliquot of liquid methanol was dropped on a cotton puff in the bottom of the luminometer tubes, allowing the release of gaseous methanol to roots or aerials parts. (B) Maximal volatile methanol-induced increases in $[Ca^{2+}]_{cyt}$ for roots and aerial parts. Data correspond to the means of at least three independent experiments ± s.d. *Significantly different from the control level before methanol addition.

unrelated anion channel inhibitors (Supplementary Data Fig. S8), as was already reported in response to oxalic acid (Errakhi *et al.*, 2008*a*). This methanol-induced ethylene production could also be reduced by inhibitors of the ACC synthase and the ACC oxidase. These data are in accordance with the methanol-induced increase in activity or gene expression of ethylene biosynthesis enzymes by methanol and other VOCs (Arimura *et al.*, 2002; Downie *et al.*, 2004; Pelloux *et al.*, 2007). In agreement with the dependence of methanol-induced anion channel regulation on $[Ca^{2+}]_{cyt}$ variations, the ethylene production was also sensitive to BAPTA and La^{3+}, as already observed in response to oxalic acid (Errakhi *et al.*, 2008*a*). Moreover this production could also be reduced by dantrolene and caffeine (Supplementary Data Fig. S8), suggesting that the $[Ca^{2+}]_{cyt}$ increase is a key upstream event in the pathway leading to methanol-induced ethylene production. The ethylene production was also recorded after volatile application of methanol to seedlings of various species (Supplementary Data Fig. S9), indicating that methanol could induce the same pathway in different species. Ethylene, like methanol, is recognized as a plant–plant volatile message controlling plant defences (von Dahl *et al.*, 2007; Broekgaarden *et al.*, 2015). In response to pathogen attack, the methanol-induced ethylene generation could thus consist of an amplification of the volatile message

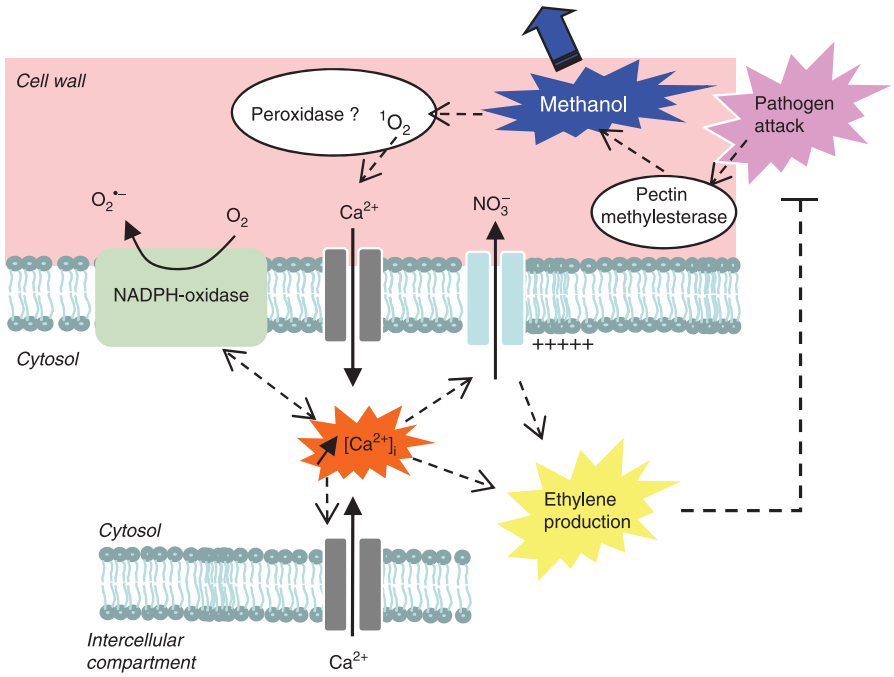

FIG. 7. Putative model for early cellular events induced by pectin methylesterase-derived methanol.

favouring information transfer between damaged and intact parts of the same plant and between plants, as was already reported for ethylene-induced release of VOCs thought to function as indirect defences (Horiuchi *et al.*, 2001; Schmelz *et al.*, 2003).

Although the amount of methanol that may accumulate in cell wall microenvironments is still to be determined, the methanol release is greatly increased through the action of pathogens (Peñuelas *et al.*, 2005; Dorokhov *et al.*, 2012) and it was shown to be emitted at much higher rates than all other detected VOCs upon feeding of larvae of *Euphydrya saurinia* on *Succisa pratensis* leaves (Peñuelas *et al.*, 2005). Taken together, our data suggest that methanol could induce $[Ca^{2+}]_{cyt}$ variations that could participate in a signalling pathway allowing plant cell response activation upon activation of PMEs. However, complementary experiments such as phenotyping experiments are needed to ascertain the role of the different players proposed in our model of methanol-induced signalling (Fig. 7).

SUPPLEMENTARY DATA

Supplementary data are available online at https://academic.oup.com/aob and consist of the following. Figure S1: effect of methanol on *Arabidopsis thaliana* cultured cell viability. Figure S2: effect of methanol on cytosolic Ca^{2+} concentration in cultured cells. Figure S3: effect of methanol on cytosolic Ca^{2+} concentration in tobacco cultured cells. Figure S4: effect of methanol on cytosolic Ca^{2+} concentration in *Arabidopsis thaliana* seedlings. Figure S5: inhibition of volatile methanol-induced increase in cytosolic Ca^{2+} concentrations of seedlings by La^{3+}. Figure S6: methanol-induced reactive oxygen species generation in BY2 cultured cells. Figure S7: methanol-induced reactive oxygen species generation in *Arabidopsis thaliana* seedlings. Figure S8: methanol-induced ethylene synthesis in *A. thaliana* cells. Figure S9: methanol-induced ethylene production in seedlings of *A. thaliana*, tobacco and sunflower.

ACKNOWLEDGEMENTS

We thank Alexis Peaucelle for his encouragement to publish these data, and Alex Demoor for checking the manuscript. We also thank the anonymous reviewers for their helpful comments. This work was supported by grants from MESRI.

LITERATURE CITED

Arimura GI, **Ozawa R**, **Nishioka T**, ***et al.* 2002**. Herbivore-induced volatiles induce the emission of ethylene in neighboring lima bean plants. *The Plant Journal* **29**: 87–98.

Asai N, **Nishioka T**, **Takabayashi J**, **Furuichi T. 2009**. Plant volatiles regulate the activities of Ca^{2+}-permeable channels and promote cytoplasmic calcium transients in Arabidopsis leaf cells. *Plant Signaling and Behavior* **4**: 294–300.

Baldwin IT, **Halitschke R**, **Paschold A**, **von Dahl CC**, **Preston CA. 2006**. Volatile signalling in plant–plant interactions: 'talking trees' in the genomics era. *Science* **311**: 812–815.

Beckers GJM, **Conrath U. 2007**. Priming for stress resistance: from the lab to the field. *Current Opinion in Plant Biology* **10**: 425–431.

Ben Hamed-Laouti I, **Arbelet-Bonnin D**, **De Bont L**, ***et al.* 2016**. Comparison of NaCl-induced programmed cell death in the obligate halophyte *Cakile maritima* and the glycophyte *Arabidopsis thaliana*. *Plant Science* **247**: 49–59.

Bewell MA, **Maathuis FJ**, **Allen GJ**, **Sanders D. 1999**. Calcium-induced calcium release mediated by a voltage-activated cation channel in vacuolar vesicles from red beet. *FEBS Letters* **458**: 41–44.

Broekgaarden C, **Caarls L**, **Vos IA**, **Pieterse CM**, **Van Wees SC. 2015**. Ethylene: traffic controller on hormonal crossroads to defense. *Plant Physiology* **169**: 2371–2379.

Camejo D, **Guzmán-Cedeño Á**, **Moreno A. 2016**. Reactive oxygen species, essential molecules, during plant–pathogen interactions. *Plant Physiology and Biochemistry* **103**: 10–23.

Carpita NC, **Gibeaut DM. 1993**. Structural models of primary cell walls in flowering plants: consistency of molecular structure with the physical properties of the walls during growth. *The Plant Journal* **3**: 1–30.

Chen YC, **Lin HH**, **Jeng ST. 2008**. Calcium influxes and mitogen-activated protein kinase kinase activation mediate ethylene inducing ipomoelin gene expression in sweet potato. *Plant, Cell and Environment* **31**: 62–72.

Cosgrove DJ. 2016. Catalysts of plant cell wall loosening. *F1000Research* **5**: 119.

von Dahl CC, **Baldwin IT. 2007**. Deciphering the role of ethylene in plant–herbivore interactions. *Journal of Plant Growth Regulation* **26**: 201–209.

von Dahl CC, **Hävecker M**, **Schlögl R**, **Baldwin IT. 2006**. Caterpillar-elicited methanol emission: a new signal in plant–herbivore interactions? *The Plant Journal* **46**: 948–960.

von Dahl CC, **Winz RA**, **Halitschke R**, **Kühnemann F**, **Gase K**, **Baldwin IT. 2007**. Tuning the herbivore-induced ethylene burst: the role of transcript accumulation and ethylene perception in *Nicotiana attenuate*. *The Plant Journal* **51**: 293–307.

Dixit S, **Upadhyay SK**, **Singh H**, **Pandey B**, **Chandrashekar K**, **Verma PC. 2013**. Pectin methylesterase of Datura species, purification, and characterization from *Datura stramonium* and its application. *Plant Signaling and Behavior* **8**: e25681.

Dorokhov YL, **Komarova TV**, **Petrunia IV**, **Frolova OY**, **Pozdyshev DV**, **Gleba YY. 2012**. Airborne signals from a wounded leaf facilitate viral spreading and induce antibacterial resistance in neighboring plants. *PLoS Pathogens* **8**: e1002640. doi: 10.1371/journal.ppat.1002640.

Downie A, **Miyazaki S**, **Bohnert H**, ***et al.* 2004**. Expression profiling of the response of *Arabidopsis thaliana* to methanol stimulation. *Phytochemistry* **65**: 2305–2316.

Duan W, **Huang Z**, **Song X**, ***et al.* 2016**. Comprehensive analysis of the polygalacturonase and pectin methylesterase genes in *Brassica rapa* shed light on their different evolutionary patterns. *Scientific Reports* **6**: 25107

Engelberth J, **Alborn HT**, **Schmelz EA**, **Tumlinson JH. 2004**. Airborne signals prime plants against insect herbivore attack. *Proceedings of the National Academy of Sciences, USA* **101**: 1781–1785.

Errakhi R, **Meimoun P**, **Lehner A**, ***et al.* 2008*a***. Anion channel activity is necessary to induce ethylene synthesis and programmed cell death in response to oxalic acid. *Journal of Experimental Botany* **59**: 3121–3129.

Errakhi R, **Dauphin A**, **Meimoun P**, ***et al.* 2008*b***. An early Ca^{2+} influx is a prerequisite to thaxtomin A-induced cell death in *Arabidopsis thaliana* cells. *Journal of Experimental Botany* **59**: 4259–4270.

Fall R, **Benson AA. 1996**. Leaf methanol – the simplest natural product from plants. *Trends in Plant Science* **9**: 296–301.

Frederickson Matika DE, **Loake GJ. 2014**. Redox regulation in plant immune function. *Antioxidants and Redox Signalling* **21**: 1373–88.

Fry SC, **Dumville JC**, **Miller JG. 2001**. Fingerprinting of polysaccharides attacked by hydroxyl radicals *in vitro* and in the cell walls of ripening pear fruit. *Biochemistry Journal* **357**: 729–737.

de Gouw JA, **Howard CJ**, **Custer TG**, **Baker BM**, **Fall R. 2000**. Proton-transfer chemical-ionization mass spectrometry allows real-time analysis of volatile organic compounds released from cutting and drying of crops. *Environmental Science and Technology* **34**: 2640–2648.

Guo W, **Ye Z**, **Wang G**, **Zhao X**, **Yuan J**, **Du Y. 2009**. Measurement of oligochitosan–tobacco cell interaction by fluorometric method using europium complexes as fluorescence probes. *Talanta* **78**: 977–982.

Haapalainen M, **Dauphin A**, **Li CM**, ***et al.* 2012**. HrpZ harpins from different *Pseudomonas syringae* pathovars differ in molecular interactions and in induction of anion channel responses in *Arabidopsis thaliana* suspension cells. *Plant Physiology and Biochemistry* **51**: 168–174.

Hann CT, **Bequette CJ**, **Dombrowski JE**, **Stratmann JW. 2014**. Methanol and ethanol modulate responses to danger- and microbe-associated molecular patterns. *Frontiers in Plant Science* **15**: 550.

Hasunuma T, **Fukusaki E**, **Kobayashi A. 2003**. Methanol production is enhanced by expression of an *Aspergillus niger* pectin methylesterase in tobacco cells. *Journal of Biotechnology* **106**: 45–52.

Harley PC, **Greenberg JP**, **Guenther AB. 2002**. ` American Geophysical Union, Fall Meeting 2002, abstract #A52D-02.

Horiuchi J, **Arimura G**, **Ozawa R**, **Shimoda T**, **Takabayashi J**, **Nishioka T. 2001**. Exogenous ACC enhances volatiles production mediated by jasmonic acid in lima bean leaves. *FEBS Letters* **509**: 332–336.

Huang YC, **Wu HC**, **Wang YD**, ***et al.* 2017**. Pectin methylesterase 34 contributes to heat tolerance through its role in promoting stomatal movement. *Plant Physiology* **174**: 748–763

Kadono T, **Tran D**, **Errakhi R**, ***et al.* 2010**. Increased anion channel activity is an unavoidable event in ozone-induced programmed cell death. *PLoS One* **5**: e13373. doi: 10.1371/journal.pone.0013373.

Kanofsky JR. 2000. Assay for singlet-oxygen generation by peroxidases using 1270-nm chemiluminescence. *Methods in Enzymology* **319**: 59–67.

Kawano T, **Sahashi N**, **Takahashi K**, **Uozumi N**, **Muto S. 1998**. Salicylic acid induces extracellular superoxide generation followed by an increase in cytosolic calcium ion in tobacco suspension culture: the earliest events in salicylic acid signal transduction. *Plant and Cell Physiology* **39**: 721–730.

Kimura M, **Kawano T. 2015**. Salicylic acid-induced superoxide generation catalyzed by plant peroxidase in hydrogen peroxide-independent manner. *Plant Signalling and Behavior* **10**: e1000145.

Kohli P, **Kalia M**, **Gupta R. 2015**. Pectin methylesterases: a review. *Journal of Bioprocessing and Biotechnique* **5**: 227.

Komarova EV, **Sheshukova EV**, **Dorokhov YL. 2014**. Cell wall methanol as a signal in plant immunity. *Frontiers in Plant Science* **5**: 101.

Knight MR, **Campbell AK**, **Smith SM**, **Trewavas AJ. 1991**. Transgenic plant aequorin reports the effects of touch and cold-shock and elicitors on cytoplasmic calcium. *Nature* **352**: 524–6.

Knight H, **Trewavas AJ**, **Knight MR. 1996**. Cold calcium signalling in Arabidopsis involves two cellular pools and a change in calcium signature after acclimatation. *The Plant Cell* **8**: 489–503.

Körner E, **von Dahl CC**, **Bonaventure G**, **Baldwin IT. 2009**. Pectin methylesterase NaPME1 contributes to the emission of methanol during insect herbivory and to the elicitation of defence responses in *Nicotiana attenuata*. *Journal of Experimental Botany* **60**: 2631–2640.

Lecourieux D, **Ranjeva R**, **Pugin A. 2006**. Calcium in plant defence-signalling pathways. *New Phytologist* **171**: 249–69.

Lehmann S, **Serrano M**, **L'Haridon F**, **Tjamos SE**, **Metraux JP. 2015**. Reactive oxygen species and plant resistance to fungal pathogens. *Phytochemistry* **112**: 54–62.

Li W, **Shang H**, **Ge Q**, ***et al.* 2016**. Genome-wide identification, phylogeny, and expression analysis of pectin methylesterases reveal their major role in cotton fiber development. *BMC Genomics* **17**: 1000.

Lionetti V, **Raiola A**, **Camardella L**, ***et al.* 2007**. Overexpression of pectinmethylesterase inhibitors in *Arabidopsis* restricts fungal infection by *Botrytis cinerea*. *Plant Physiology* **143**: 1871–1880.

Lionetti V, **Cervone F**, **Bellincampi D. 2012**. Methylesterification of pectin plays a role during plan–pathogen interactions and affects plant resistance to diseases. *Journal of Plant Physiology* **169**: 1623–1630.

Lionetti V, **Fabri E**, **De Caroli M**, ***et al.* 2017**. Three pectin methylesterase inhibitors protect cell wall integrity for Arabidopsis immunity to Botrytis. *Plant Physiology* **173**: 1844–1863.

Liu J, **Knight H**, **Hurst CH**, **Knight MR. 2012**. Modelling and experimental analysis of the role of interacting cytosolic and vacuolar pools in shaping low temperature calcium signatures in plant cells. *Molecular Biosystems* **8**: 2205–2220.

Ma W. 2011. Roles of Ca^{2+} and cyclic nucleotide gated channel in plant innate immunity. *Plant Science* **181**: 342–346.

Maffei ME, **Mithöfer A**, **Boland W. 2007**. Insects feeding on plants: rapid signals and responses preceding the induction of phytochemical release. *Phytochemistry* **68**: 2946–2959.

Meimoun P, **Vidal G**, **Bohrer AS**, ***et al.* 2009*a***. Intracellular Ca^{2+} stores could participate to abscisic acid-induced depolarization and stomatal closure in *Arabidopsis thaliana*. *Plant Signaling and Behavior* **4**: 830–835.

Meimoun P, **Tran D**, **Baz M**, ***et al.* 2009*b***. Two different signaling pathways for thaxtomin A-induced cell death in Arabidopsis and tobacco BY2. *Plant Signaling and Behavior* **4**: 142–144.

Monetti E, **Kadono T**, **Tran D**, ***et al.* 2014**. Deciphering early events involved in hyperosmotic stress-induced programmed cell death in tobacco BY-2 cells. *Journal of Experimental Botany* **65**: 1361–75.

Nagano M, **Ishikawa T**, **Fujiwara M**, ***et al.* 2016**. Plasma membrane microdomains are essential for Rac1-RbohB/H-mediated immunity in rice. *The Plant Cell* **28**: 1966–1983.

Nakano N, **Sugioka K**, **Ushijima Y**, **Goto T. 1986**. Chemiluminescence probe with *Cypridina* luciferin analog, 2-methyl-6-phenyl-3,7-dihydroimidazo[1,2-a]pyrazin-3-one, for estimating the ability of human-granulocytes to generate O_2^-. *Annals of Biochemistry* **159**: 363–369.

Nemecek-Marshall M, **MacDonald RC**, **Franzen JJ**, **Wojciechowski CL**, **Fall R. 1995**. Methanol emission from leaves. *Plant Physiology* **108**: 1359–1368.

Nguyen HP, **Jeong HY**, **Jeon SH**, **Kim D**, **Lee C. 2017**. Rice pectin methylesterase inhibitor28 (OsPMEI28) encodes a functional PMEI and its overexpression results in a dwarf phenotype through increased pectin methylesterification levels. *Journal of Plant Physiology* **208**: 17–25.

Pelloux J, **Rustérucci C**, **Mellerowicz EJ. 2007**. New insights into pectin methylesterase structure and function. *Trends in Plant Science* **12**: 267–277.

Peñuelas J, **Filella I**, **Stefanescu C**, **Llusià J. 2005**. Caterpillars of *Euphydryas aurina* (Lepidoptera: Nymphalidae) feeding on *Succisa pratensis* leaves induce large foliar emissions of methanol. *New Phytologist* **167**: 851–857.

Pickett JA, **Khan ZR. 2016**. Plant volatile-mediated signalling and its application in agriculture: successes and challenges. *New Phytologist* **212**: 856–870.

Pogány M, **von Rad U**, **Grün S**, ***et al.* 2009**. Dual roles of reactive oxygen species and NADPH oxidase RBOHD in an *Arabidopsis–Alternaria* pathosystem. *Plant Physiology* **151**: 1459–1475.

Pottosin I, **Shabala S. 2014**. Polyamines control of cation transport across plant membranes: implications for ion homeostasis and abiotic stress signaling. *Frontiers in Plant Science* **5**: 154.

Raiola A, **Lionetti V**, **Elmaghraby I**, ***et al.* 2011**. Pectin methylesterase is induced in Arabidopsis upon infection and is necessary for a successful colonization by necrotrophic pathogens. *Molecular Plant-Microbe Interactions* **24**: 432–440.

Ramirez I, **Dorta F**, **Espinoza V**, **Jimenez E**, **Mercado A**, **Pena-Cortes H. 2006**. Effects of foliar and root applications of methanol on the growth of Arabidopsis, tobacco, and tomato plants. *Journal of Plant Growth Regulation* **25**: 30–44.

Reboutier D, **Bianchi M**, **Brault M**, ***et al.* 2002**. The indolic compound hypaphorine produced by ectomycorrhizal fungus interferes with auxin action and evokes early responses in non-host *Arabidopsis thaliana*. *Molecular Plant-Microbe Interactions* **15**: 932–938.

Reboutier D, **Vedel R**, **Brault M**, ***et al.* 2005**. A CFTR chloride channel activator prevents $HrpN_{ea}$-induced cell death in *Arabidopsis thaliana* suspension cells. *Plant Physiology and Biochemistry* **43**: 567–572

Reignault P, **Valette-Collet O**, **Boccara M. 2008**. The importance of fungal pectinolytic enzymes in plant invasion, host adaptability and symptom type. *European Journal of Plant Pathology* **120**: 1–11.

Schmelz EA, **Alborn HT**, **Tumlinson JH. 2003**. Synergistic interactions between volicitin, jasmonic acid and ethylene mediate insect-induced volatile emission in *Zea mays*. *Physiologia Plantarum* **117**: 403–412.

Schopfer P. 2001. Hydroxyl radical-induced cell-wall loosening *in vitro* and *in vivo*: implications for the control of elongation growth. *The Plant Journal* **28**: 679–688.

Seybold H, **Trempel F**, **Ranf S**, **Scheel D**, **Romeis T**, **Lee J. 2014**. Ca^{2+} signalling in plant immune response: from pattern recognition receptors to Ca^{2+} decoding mechanisms. *New Phytologist* **204**: 782–790.

Tenhaken R. 2015. Cell wall remodeling under abiotic stress. *Frontiers in Plant Science* **5**: 771.

Tran D, **El-Maarouf-Bouteau H**, **Rossi M**, ***et al.* 2013**. Post-transcriptional regulation of GORK channels by superoxide anion contributes to increase in outward-rectifying K^+ currents. *New Phytologist* **198**: 1039–1048.

Volpi C, **Janni M**, **Lionetti V**, **Bellincampi D**, **Favaron F**, **d'Ovidio R. 2011**. The ectopic expression of a pectinmethylesterase inhibitor increases pectin methylesterification and limits fungal diseases in wheat. *Molecular Plant-Microbe Interaction* **24**: 1012–1019.

Vorwerk S, **Somerville S**, **Somerville C. 2004**. The role of plant cell wall polysaccharide composition in disease resistance. *Trends in Plant Science* **9**: 203–209.

Walter A, **Mazars C**, **Maitrejean M**, ***et al.* 2007**. Structural requirements of jasmonates and synthetic analogues as inducers of Ca^{2+} signals in the

nucleus and the cytosol of plant cells. *Angewandte Chemie International Edition* **46**: 4783–4785.

Wolf S, **Greiner S. 2012**. Growth control by cell wall pectins. *Protoplasma* **249** (Suppl 2): S169–S175.

Wu HC, **Jinn TL. 2010**. Heat shock-triggered Ca^{2+} mobilization accompanied by pectin methylesterase activity and cytosolic Ca^{2+} oscillation are crucial for plant thermotolerance. *Plant Signaling and Behavior* **5**: 1252–1256.

Wu S, **Shan L**, **He P. 2014**. Microbial signature-triggered plant defense responses and early signalling mechanisms. *Plant Science* **228**: 118–126.

Xia Y, **Petti C**, **Williams MA**, **DeBolt S. 2014**. Experimental approaches to study plant cell walls during plant–microbe interactions. *Frontiers in Plant Science* **5**: 540.

Zebelo SA, **Matsui K**, **Ozawa R**, **Maffei ME. 2012**. Plasma membrane potential depolarization and cytosolic calcium flux are early events involved in tomato (*Solanum lycopersicon*) plant-to-plant communication. *Plant Science* **196**: 93–100.

Zhang L, **Du L**, **Poovaiah BW. 2014**. Calcium signalling and biotic defense responses in plants. *Plant Signaling and Behavior* **9**: e973818.

Zhang HM, **van Helden DF**, **McCurdy DW**, **Offler CE**, **Patrick JW. 2015**. Plasma membrane Ca^{2+}-permeable channels are differentially regulated by ethylene and hydrogen peroxide to generate persistent plumes of elevated cytosolic Ca^{2+} during transfer cell trans-differentiation. *Plant and Cell Physiology* **56**: 1711–1720.